GL04123

Gamma-Ray Spectrometry in Geological Mapping and in Uranium Exploration

by

*Stanley H. Ward

* Department of Geology and Geophysics,
University of Utah, and Earth Science Laboratory,
University of Utah Research Institute

Abstract

Gamma-ray spectrometry, airborne or ground, may be useful in a wide variety of geologic mapping applications because the concentrations of uranium, thorium and/or potassium may be diagnostic of rock type in many uranium, base and precious metal environments. However, in areas of little outcrop, the surface material must be either residual or locally derived before gamma-ray spectrometry can be applied successfully. In its alternate application, direct detection of uranium, gamma-ray spectrometry has been remarkably successful in recent years. However, for direct detection of uranium deposits, gamma-ray spectrometry will decrease application because most deposits occurring sufficiently close to surface to be detected have already been found.

To be of maximum use to the explorationist, data from gamma-ray spectrometry surveys must be acquired with utmost care. Accordingly, attention must be directed to evaluation of such problems as: disequilibrium in the uranium decay series, removal of atmospheric background radiation, the effect of rainfall and of other meteorological phenomena, calibration of spectrometers, statistical errors in count rates, fields of view of gamma-ray detectors, and the effect of overburden. Modern instrumentation, calibration, and analysis are such that these problems can be evaluated with such care that as little as 1 ppm U, 1 ppm Th, or 0.1% K can be detected reliably with an airborne or ground gamma-ray spectrometry survey.

Introduction

There are two objectives of gamma-ray spectrometry: *direct detection* of uranium deposits and *geological mapping* by detecting and delineating the lateral distribution of uranium, thorium, and potassium in surface rocks and soils. Gamma-ray spectrometry was successful, for example, in recent discoveries of the Ranger, Koongarra, and Nabarlek deposits in Northern Territory, Australia, and of the Cluff Lake and Rabbit Lake deposits in Saskatchewan, Canada (Armstrong and Brewster, 1979). However, for direct detection of uranium deposits, gamma-ray spectrometry is decreasing in importance because it virtually demands the occurrence of uranium or its radioactive decay products within 0.20 m to 0.45 m of the surface; most such deposits have been found or soon will have been found. Hence geologic mapping ought to be the principal objective of gamma-ray spectrometry. This type of geologic mapping may be useful indirectly in the search for base metal ores of copper, lead, and zinc, as well as in detecting and delineating uranium-rich source rocks in which uranium deposits occur or from which uranium deposits may be derived (Moxham et al., 1965; Pitkin, 1968; Davis and Guilbert, 1973; Schwarzer and Adams, 1973). Use of a gamma-ray spectrometer will be most effective in mapping those acid igneous rocks, zones of potassium metasomatism, shales, sandstones, carbonates, and evaporites in which uranium, thorium, and/or potassium are enriched. Basic igneous and sedimentary rocks of low uranium, thorium and/or potassium content are not so easily distinguished from one another by this method. Table 1 lists the mean concentrations of uranium, thorium, and potassium for the rock types referenced above.

Concentrations of uranium, thorium and potassium vary sympathetically in many geologic materials. However, selective concentration or depletion of

each of these elements occurs in certain geologic processes. Thus for many geologic materials, the integrated gamma radiation arising in the uranium, thorium, and potassium radioactive decay processes is sufficient as an indicator of rock type, while in other geologic materials, gamma radiation specific to uranium, thorium, and potassium may be may be necessary to distinguish rock types. In areas of little outcrop, the surface material must be reasonably representative of the underlying bedrock and must be either residual or locally derived before gamma-ray spectrometry can be applied successfully. The usefulness of radioactivity surveys for geologic mapping will therefore vary from place to place, depending upon the nature of the overburden.

Standard reference texts to which the reader might wish to refer for discussion of the principles of gamma-ray spectrometry include Crouthamel (1969), Adams and Gasparini (1970), and Kogan et al. (1971). Useful reference collections of papers on applications of gamma-ray spectrometry appear in proceedings of symposia organized by the International Atomic Energy Agency (1973) and (1976).

Natural Radioactive Decay Processes

Elementary Particles

Radioactive decay is a statistical process in which the number of atoms that disintegrate per unit time is proportional to the number of atoms present. A few nuclides are radioactive and decay to produce other nuclides; ^{40}K, ^{238}U, ^{235}U, and ^{232}Th are the most important of these. Most nuclear transformations involve emissions of alpha particles (α), beta particles (β), and gamma-rays (γ). Two other forms of atomic transformation are electron capture and spontaneous nuclear fission. Radioactive decay is an exothermic

process in which the excess energies of the unstable nuclei are carried away through the emission of α, β and γ. Gamma-ray emission does not occur as an independent form of radioactivity but is part of α and β decay processes. Gamma-rays are high-energy electromagnetic radiation emitted by an excited nucleus as it drops to a less excited state.

Gamma-rays are emitted in packets or *quanta* of energy called photons. The energy E of each photon depends upon its characteristic wavelength γ or frequency ν and is given by

$$E = h\nu = h\, c/\lambda$$

where h is Planck's constant and c is the velocity of light. Energies are usually expressed in *electron volts* (e.v.). One electron volt is the energy acquired by a charged particle carrying unit electronic charge when it is accelerated through a potential difference of one volt. Gamma-rays exhibit frequencies of 10^{19} to 10^{21} sec^{-1}, wavelengths of 10^{-11} to 10^{-13} m, energies of 40 KeV to 4 MeV where K stands for 10^{3} and M stands for 10^{6}.

Alpha particles are absorbed by a few centimeters of air, β particles by a meter or so of air, while high energy γ-radiation will travel several hundred meters through air. Their equivalent ranges in rock are practically zero for α and β particles and about 0.20 m to 0.45 m for γ-rays depending on the energy of the latter. These observations dictate that radioactive decay processes are only realistically monitored in the field by γ-ray detectors, except for the detection of decay products such as Rn gas (Pedersen et al., 1979).

The uranium isotope $^{238}_{92}U$ decays to stable $^{206}_{82}Pb$ through 17 intermediate daughter products as shown in Table 2. In the process, gamma-rays of 72 discrete energy levels are emitted. The most energetic or the principal gamma lines of this spectrum are listed in Table 3. The ratio of the total gamma-

ray energy of ^{238}U and ^{235}U, in the natural state, is approximately 50:1 so that the ^{235}U lines are of subsidiary interest to the ^{238}U lines.

The thorium isotope $^{232}_{90}Th$ decays to stable $^{208}_{82}Pb$ through ten intermediate daughter products as shown in Table 4. In the process, gamma-rays of 46 discrete energy levels are emitted. The principal lines of this spectrum are listed in Table 5.

The potassium isotope ^{40}K emits gamma-rays of 1.46 MeV through electron capture; 0.012 percent of potassium is ^{40}K.

When uranium, thorium and potassium are all present, the composite spectrum might look like that displayed in Figure 1 in which the individual lines have been broadened into peaks by the low resolution thallium-activated sodium iodide crystal used in the detection instrument.

Equilibrium and disequilibrium

At equilibrium the number of atoms of each daughter product disintegrating per second is the same as the number being created by disintegrations of the parent.

In the case of a radioactive decay series with n products, the time to reach equilibrium is less thn 100 years for the thorium decay process and is about 10^6 years for the two uranium decay processes; the time required for establishing equilibrium is determined by the half-life of the isotope of longest life.

Measurement of gamma-radiation associated with daughter products in a decay process in which equilibrium has been established permits determining the parent amount by measuring the daughter amount. Thus it has become recent practice to measure four quantities in gamma-ray spectrometry. These four

quantities are:

TC = Total count integrated under the spectrum between 0.4 MeV and 2.82 MeV.

^{40}K = Radioactive potassium content via integrated count between 1.36 MeV and 1.56 MeV (the so-called 1.46 MeV ^{40}K peak of Figure 1).

^{238}U = Uranium via integrated count between 1.66 MeV and 1.86 MeV (the so-called 1.76 MeV ^{214}Bi peak of Figure 1).

^{232}Th = Thorium via integrated count between 2.42 MeV and 2.82 MeV (the so-called 2.62 MeV ^{208}Tl peak of Figure 1).

One should note from Table 2 that ^{214}Bi is many steps removed from ^{238}U and that the intermediate daughter products include radium and radon. The solubility of radium is different from that of uranium so that radium can separate from uranium in common geologic processes. Radon is a light gas which emanates from the earth's surface and so also readily separates from uranium. Therefore, in an open environment, ^{214}Bi may be spatially separated from its parent ^{238}U through migration of earlier daughter products in the decay process. For this reason, an estimation of the abundance of uranium based on a measurement of ^{214}Bi is correct only if the radioactive decay process is in equilibrium.

Scattering and absorption

When gamma photons pass through matter, they interact with the electrons and with the acomic nuclei of the matter via various mechanisms. These mechanisms can be divided into a) elastic interactions in which the photon does not transfer its energy to other particles, known as Thomson scattering, and b) inelastic interactions in which the photon either loses part of its energy and is deflected from its initial direction or gives up all of its

energy to an atomic electron or nucleus and ceases to exist. For photons with energies from a few KeV to a few MeV, the important inelastic interactions are the nuclear photoelectric effect, formation of electron-positron pairs, the photoelectric effect, and Compton scattering.

When a beam of collimated mono-energetic photons passes through an absorber, the numbr of photons per cm^2 per sec (N) at the plane defined by x is given by

$$N = N_0 e^{-\mu x}$$

where N_0 is the incident flux at $x = 0$, μ and is the total absorption coefficient due to the photoelectric effect, Compton scattering, and pair production. The thickness of the material that reduces the intensity N to half of N_0 is referred to as the half-thickness. For $N/N_0 = 1/2$, we find $x = \frac{\ln(2)}{\mu}$ from the previous equation. Table 6 shows the half-thickness at various energies for water, air at 20°C and 76 cm Hg, and for rock of density 2.35 gm/cm^3. As expected, photons of higher energy penetrate farthest.

Ninety percent of the gamma-rays observed at the surface of rock outcrop of density 2.7 gm/cm^3 are emitted from the top 0.15 to 0.25 m while 90% of the gamma-rays observed at the surface of dry overburden of 1.5 gm/cm^3 are received from the top 0.30 to 0.45 cm. Moisture in the soil increases the attenuation significantly.

Operational Considerations

Background

The discrete spectral lines that provide information on the radionuclide abundances are degraded by the Compton continuum, the *background radiation*. The latter arises from 1) ^{40}K contamination in the crystal, b) ^{238}U, ^{232}Th,

and ^{40}K contamination in the materials used in constructing photomultiplier tubes (the gamma-ray detector) and the crystal/photomultiplier tube (PMT) housing, c) radioactive accumulations on or in the aircraft structure (for airborne systems), d) radium luminized instruments e.g., navigation instruments in airborne surveys and watches in ground surveys, e) cosmic ray interactions with nuclei present in the air, the aircraft, or the detector, and f) atmospheric radioactivity arising from daughter products of radon gas of the uranium decay series.

Every effort must be expended in ground and airborne surveys to minimize background radiation and to remove it prior to attempting to utilize spectrometer data for estimates of nuclide concentrations.

Careful quality control of materials selected for detector, and PMT and housing can usually keep contamination in these items to an acceptable level. However, background from the detector may contribute as much as 50 counts per second within the ^{214}Bi window for a 3072 cu.in. (5.0×10^4 cc) crystal array. That same level, approximately, is the ^{214}Bi channel count from a half-space located 125 m beneath the aircraft and containing 5 ppm uranium.

Radioactive nuclides can precipitate and adhere to the skin of an aircraft, be contaminants in aircraft materials, be used to illuminate instruments, or occur in luminescent strips or signs on the aircraft. The aircraft should be checked for these sources with a hand-held spectrometer and the offending nuclides removed where possible. Crystal detectors should be placed sufficiently far from the instrument panel, after reduction of panel luminescence to low level, that the remaining luminescence is insignificant within the energy windows studied. Periodic checks of the aircraft with a hand-held spectrometer are customary.

Cosmic-rays are fast moving charged particles of extraterrestrial origin. One type of cosmic-ray is dominated by time-variant fluxes of particles are energy and it is always present at the earth's surface. These particles of high believed to originate in our galaxy and to be distributed throughout it; they are referred to as *galactic cosmic-rays*. The galactic cosmic-rays interact with the earth's atmosphere via nuclear and electromagnetic processes with a resultant loss in cosmic-ray intensity. Secondary particles produced in the interactions, readily detected at the earth's surface, increase in intensity from the equator to the auroral zones. Gamma photons covering the complete spectrum of our interest (i.e., 0.4 to 3.0 MeV) arise as a result of the secondary particles. Indeed, the secondary radiation extends to about 6.0 MeV, a fact that permits us to extrapolate the 6.0 MeV to 3.0 MeV flux to the 3.0 MeV to 0.40 MeV range to effect subtraction of cosmic radiation from the 0.4 MeV to 3.0 MeV spectrum. The intensity of cosmic radiation increases with altitude.

Background radiation emanating from the daughter products in the uranium decay series is a subject that requires substantial elaboration because this radiation can be intense and is intensely time-variant; it will be the subject of a special discussion under *meteorological effects*.

Meteorological effects

Atmospheric Bismuth 214: Radon, with a half-life of 3.8 days, can diffuse from the ground with a rate dependent upon air pressure, soil moisture, ground cover, wind, and temperature. Radon decays to ^{214}Bi, the uranium indicator in gamma-ray spectrometry. A temperature inversion in the atmosphere finds temperature increasing with altitude. Under this condition the ^{214}Bi will accumulate near the earth's surface (Foote, 1969). Anomalous uranium indications will occur, on this account, which have no relation to the

uranium content of rocks and soils beneath the detector. Darnley et al. (1968) report that, on the average, 70 percent of the counts in the uranium window arise from this source. Removal of such background becomes mandatory.

The above effect is particularly worrisome in hilly terrain where, in still air, the inversion will be pronounced in the valleys. One can presume that this effect will be minimized when breezes homogenize the air about the mid-morning of a still day, but there is no means to preduct the magnitude of the atmospheric inversion problem. The inversion layer may be entirely absent during several months of the year depending upon local climatology. Further, it may readily be a local and seasonal phenomenon, occurring in some valleys and not in others.

Thunderstorms bring increased air conductivity which can lead to removal of charged particles with which some atmospheric radiation is associated.

Attempts to minimize the atmospheric effect, by subtracting for each energy window the gamma counts of the background measured by an upward-looking detector shielded by 0.10 m of lead from ground radiation, are used in some airborne surveys. However, because the atmosphere above and below the aircraft will, in general, have different radon concentrations, this correction is imperfect and can be misleading. It removes, however, the cosmic flux. Flying over a large body of water before and after each flight aids materially in recognizing and therefore permitting elimination of, atmospheric background since water contains negligible concentrations of radioactive nuclides. Since atmospheric background is time-variant, every opportunity should be taken to fly over an extended body of water *during* as well as at the beginning and end of each flight. For ground surveys with hand-held spectrometers, background can be measured by holding the spectrometer over water of 1 m or more in depth. Finally, for airborne

surveys, the aircraft should be taken to terrain clearances of 1000 m or more where background is present but where the ground radiation is reduced to neglibible proportions through absorption in the air.

Rainfall: The following effects of rainfall have been observed:

1) moisture increases the attenuation in an energy-dependent manner and hence leads to skewing of the observed spectrum towards the high energy gamma-rays,

2) radioactive elements and their daughter products can be removed selectively over local areas by rapid runoff of rain,

3) some nuclides may not reach the top 0.20 m to 0.45 m, the zone of radiation, because of downward percolation due to rain

4) extra moisture in the soil may prevent radon from escaping to the atmosphere so that the ground contribution to the ^{214}Bi window is reduced, and

5) rain may wash ^{214}Bi from the atmosphere and hence reduce background in the channel selected to detect ^{238}U.

These effects are interrelated and are not completely understood. Experience to date indicates that recovery to pre-rainfall conditions may take place in several hours, but the recovery time is peculiar to every climatic and physiographic area on earth. Drainage of soils, atmospheric inversions, barometric pressure, and amount and lateral extent of rainfall are all to be considered in evaluating this problem. The data of Figure 2 were obtained from long-term monitoring of the gamma-ray flux at Dallas, Texas, but while peculiar to a specific area, they can serve as a guide to recovery to pre-rainfall conditions.

Calibration of Gamma-Ray Spectrometers

Recent articles that describe ground and airborne gamma-ray spectrometer calibration include Grasty (1976), Løvborg et al. (1977), Ward and Stromswold (1978), and Kirton and Lyus (1979).

Some counts will be recorded in the lower energy uranium and potassium windows due to Compton scattering in the ground, in the air, or in the detector, from a pure thorium source. Similarly, counts will be recorded in the lower energy potassium window from a pure uranium source. Table 7 illustrates these features. The ratio of the counts in a lower energy window to those in a higher energy window from a pure uranium or thorium source is termed a stripping ratio or spectral stripping coefficient. These coefficients are peculiar to each detector system.

The purpose of calibration is to convert the recorded count rates into equivalent ground concentrations of potassium uranium, and thorium. To do this, it is necessary to know the Compton stripping ratios and their variation with altitude, the height attenuation coefficients, and the sensitivities of the spectrometer for airborne systems. For ground systems the altitude variability of the Compton stripping ratios and the height attenuation coefficients are unimportant. If the calibration is performed correctly, then *assaying* by gamma-ray spectrometry can predict concentration of the principal radionuclides to accuracies of better than 1 ppm uranium, 1 ppm thorium, and 0.1% potassium for either an airborne or a ground system.

The equations that permit us to obtain thorium, uranium, and potassium concentrations from thorium, uranium and potassium channel counts, after correction for background and Compton scattering, are

$$T_U - T_B = k_1 \; T \text{ ppm},$$

$$U_U - U_B - \alpha(T_U - T_B) = k_2 \; U \text{ ppm},$$

and

$$K_U - K_B - \beta(T_U - T_B) - \{\gamma(U_U - U_B) - \alpha(T_U - T_B)\} = k_3 k \text{ pct},$$

in which T_U, U_U and K_U are uncorrected or observed count rates for the Th, U, and K channels. T_B, U_B, and K_B are background count rates, α, β, and γ are the Compton stripping ratios, while k_1, k_2 and k_3 are the thorium, uranium, and potassium sensitivities. Calibration involves determination of the nine quantities: T_B, U_B, K_B, α, β, γ, k_1, k_2, and k_3. .

Statistical errors in count rates

The error in a gamma-ray count is usually estimated by computing one standard deviation (1σ) as (Darnley et al., (1968)

$$1\sigma = \pm\sqrt{N}$$

where N is the Compton-corrected count for any given time interval, and 1σ represents the 68% confidence level, assuming a normal distribution.

The above estimates of percent standard deviation are only satisfactory if any one of K, U, or Th occurs alone and without background or Compton scattering. When the latter two effects are both present and corrections for both have been made, there is greater uncertainty in any one count rate, and hence we should use (Darnley et al., 1968)

$$\sigma_{Th} = \pm\left[N^o_{Th} + N^b_{Th}\right]^{1/2} ,$$

$$\sigma_U = \pm\left[N^o_K + N^b_K + \alpha^2\sigma^2_{Th}\right]^{1/2} ,$$

and

$$\sigma_K = \pm\left[N^o_K + N^b_K + \beta^2\sigma^2_{Th} + \gamma^2\sigma^2_U\right]^{1/2} ,$$

in which the superscripts o and b refer to observed and background respectively, and in which α, β, and γ are the Compton scattering

Coefficients, and N_{Th}, N_U, and N_K are the counts per unit time in the thorium, uranium, and potassium windows, respectiveley.

Fields of view of gamma-ray detectors

An airborne gamma-ray detector receives ground radiation from horizon to horizon, a total angle of 180 degrees. It can be established that 66 percent of the counts come from an area of diameter approximately equal to twice the terrain clearance as illustrated in Figure 3a.

Figures 3b through 3d show the effect of topography on count rates, observed with an airborne detector, over ridges and valleys. The valley or the ridge can produce either a low or a high count rate depending upon adherence to or deviation from nominal terrain clearance.

The probability of detecting a uranium deposit with an airborne gamma-ray detector is not large. Figure 4 illustrates the geometry of the problem; a thin strip of highly radioactive material oriented normal to the flight line, ideally, occurs within a circular *field of view* of the detector. The anomaly observed by a stationary detector is then

$$\text{STATIC ANOMALY} = \frac{(\pi H^2 - HW)C_1 + HWC_2}{\pi H^2 C_1}$$

$$= \frac{(\pi H - W) + WC_2/C_1}{\pi H}$$

whereas the anomaly observed by a moving detector is

$$\text{DYNAMIC ANOMALY} = \frac{\left[\pi(\frac{H}{2})S - (\frac{H}{2})W\right]C_1 + (\frac{H}{2})WC_2}{(\frac{H}{2})SC_1}$$

$$= \frac{(\pi S - W) + WC_2/C_1}{\pi S}$$

wherein the dynamic detection width H/2 is given as half its static value H. This is done "because in integrating the detector response of circular sources along the flight line, the same point on the ground is in effect sampled many times, and points closer to the flight line repeatedly generate a greater contribution to the detected count rate than do those far away" (Grasty et al., 1979). This article also establishes that the reduction in swath width ranges between 1/3 and 2/3 of the diameter similarly influenced by the stationary detector. We shall adopt a value of 1/2.

If we postulate a deposit 10 m wide by 150 m length, striking normal to the flight line, and containing U_3O_8 in concentration 100 times background, then the *static anomaly* is given by curve a) of Figure 5. The ratio of anomaly to background ranges from 13.6 for 25 m flight altitude to 3.1 for 150 m flight altitude; statistical and other uncertainties could readily obscure anomalies at altitudes of 100 m and greater. The *dynamic anomaly* over the same deposit appears as curves b) and c) for 1.0 sec and 2.5 sec integration times, respectively, for an aircraft travelling at 200 km/hr. Clearly, aircraft speed and integration time affect the ability of an airborne system to detect a surface deposit.

If a hand specimen is held at a distance of 0.25 m to 0.50 m from a spectrometer having a crystal size of, say, 347 cc, it will subtend a solid angle at the detector of much less than 90 degrees. Hence, if the half-space response formula for U, Th, or K concentration versus counts is to be used to estimate concentration, then the hand specimen must be held directly on the flat end face of the spectrometer and should be larger than the end face to approximate the same recording conditions.

The effect of overburden

If the overburden is residual, radiation from it in many cases will be

representative of the bedrock, depending upon the weathering processes. Transported overburden may produce radiation entirely misrepresentative of the bedrock.

Applications

Deposit Detection

Figure 6 portrays the results of a single traverse of a typical high quality gamma-ray spectrometric survey performed in the Northern Territory, Australia. The figure and its caption indicate a broad total count radiometric anomaly occurs between points A and B. Over this total interval of about 4 km, the potassium and thorium counts are high. On the other hand, the uranium counts are only high near point B. If the *uranium counts* near point B are indicative of commercial mineralization, then the *total count* data would not have drawn specific attention to it and would have suggested a broad radioactive source. The advantage of gamma-ray spectrometry, as opposed to total count surveys, is clearly established by this example. The ratio data of channels 3 and 4 provide very little additional information; hence their recording seems unnecessary for this particular survey.

Geological mapping

Figure 7, also from Northern Territory, Australia, reveals excellent mapping of the three basic geologic units by the potassium count channel. The granite is of Middle Proterozoic age and is intrusive into the shales of the Lower Proterozoic Arunta formation. The Central Mount Stewart Beds, of Upper Proterozoic age, are locally sandstones overlying the Arunta formation. The counts in thorium and uranium channels and the U/K and U/Th ratios are not nearly as effective as the potassium channel counts in identification of contact locations in this region of minimal fresh outcrop.

Interestingly, the uranium channel indicates clearly a sharp peak at the contact between the Arunta formation and the granite. A contact metaphorphic uranium deposit, economic or otherwise, is thus identified at this location.

FIGURE CAPTIONS

Fig. 1 Gamma-ray spectrum observed with a 1024 cu. in. (16.8×10^3 cc) crystal detector over a mix of K, Th, and U sources (courtesy GeoMetrics).

Fig. 2 ^{214}Bi counting rate recovery times back to pre-rainfall conditions versus rainfall, Dallas, TX (after Saunders and Potts, 1978).

Fig. 3 The effect of source geometry upon count rate (after Grasty, 1976).

Fig. 4 Fields of view of a) static airborne detector, and b) dynamic (or moving) detector.

Fig. 5 Ratio of anomaly to background for a) static case, b) dynamic case with 1 sec. integration time, and c) dynamic case with 2.5 sec. integration time.

Fig. 6 Airborne radiometric data obtained in the Northern Territory, Australia, with a 2000 cu. in. crystal at 80 m altitude. The data recorded, on each of the eight channels of information, is labeled on the left-hand side of the diagram. This figure illustrates the concept of deposit detection by airborne gamma-ray spectrometry (courtesy C. R. A. Exploration Pty. Ltd.).

Fig. 7 Airborne radiometric data obtained in the Northern Territory, Australia, with a 2000 cu. in. crystal at 80 m altitude. The data recorded, on each of the eight channels of information, is labeled on the left-hand side of the diagram. This figure illustrates the concept of geological mapping, coincidental deposit detection, by airborne gamma-ray spectrometry (courtesy C. R. A. Exploration Pty. Ltd.).

REFERENCES

Adams, J. A. S., Osmond, J. K., and Rogers, J. J. W., 1959, The geochemistry of thorium and uranium; *in* L. H. Ahrens, F. Press, K. Rankama, and S. K. Runcorn (eds.), Physics and Chemistry of the Earth, v. 3: New York, Pergamon Press, p. 298-348.

Adams, J. A. S., and Gasparini, P., 1970, Gamma-ray spectrometry of rocks: Elsevier Publishing Company, New York, 295 p.

Armstrong, C. W., and Brewster, N. E., 1979, A comparison of exploration techniques for uranium deposits occurring in Saskatchewan and the Northern Territory, Extended Abstracts: Internat. Uranium Sympos. on the Pine Creek geosyncline, Australia, p. 4-7.

Crouthamel, C. E., ed., 1969, Applied gamma-ray spectrometry, New York, Pergammon Press Inc. 443 p.

Darnley, A. G., Bristow, Q., and Donhoffer, D. K., 1968, Airborne gamma-ray spectrometer experiments over the Canadian Shield *in* Nuclear Technology and Mineral Resources: Internat. Atomic Energy Agency, Vienna, P. 163-186.

Davis, J. D., and Guilbert, J. M., 1973, Distribution of Radioelements Potassium, Uranium, and Thorium in Selected Porphyry Copper Deposits: Econ. Geol., v. 68, p. 145-160.

Foote, R. S., 1969, Improvement in airborne gamma-radiation analyses for anomalous radiation by removal of environmental and pedologic radiation changes *in* Proc. Symp. on Use of Nuclear Techniques in the Prospecting and development of Mineral Resources: Internat. Atomic Energy Agency, Vienna.

Grasty, R. L., 1976, A calibration procedure for an airborne gamma-ray spectrometer: Geol. Surv. Can. Prof. Paper 76-16.

Grasty, R. L., Kosanke, K. L., and Foote, R. S., 1979, Fields of view of airborne gamma-ray detectors: Geophysics, v. 44, p. 1447-1457.

International Atomic Energy Agency, 1973, Uranium Exploration Methods: UNIPUB, New York.

International Atomic Energy Agency, 1976, Exploration for Uranium Ore Deposits: UNIPUB, New York, 807 p.

Kirton, M., and Lyus, D., 1979, Calibration of an airborne gamma-ray spectrometer over Mary Kathleen Mine: Bull. Aust. Soc. of Exp. Geophys., v. 10, p. 69-74.

Kogan, R. M., Nazarov, I. M., and Fridman, Sh. D., 1971, Gamma spectrometry of natural environments and formations, Moscow: Atomizdat, translated from the Russian by the Israel Program for Scientific Translations, Jerusalem, 337 p.

Løvborg, L., Grasty, R. L., and Kirkegaard, P., 1977, A guide to the calibration constants for aerial gamma-ray surveys in geoexploration,

paper presented at American Nuclear Society Symposium: Aerial Techniques for Environmental Monitoring, Las Vegas, Nevada.

Moxham, R. M., Foote, R. S., and Bunker, C. M., 1965, Gamma-ray spectrometer studies on hydrothermally altered rocks: Economic Geology, v. 60, p. 653-671.

Pedersen, G. P., Dunbier, J., and Gingrich, J. E., 1979, Experience with track etch method for uranium exploration in northern Australia: Extended Abstracts, Internat. Uranium Sympos. on the Pine Creek geosyncline, Australia, p. 159-162.

Pitkin, J. A., 1968, Airborne measurements of terrestrial radioactivity as an aid to geologic mapping: USGS Prof. Paper 516-F, 29 p.

Schwarzer, T. F., and Admas, J. A. S., 1973, Rock and soil discrimination by low altitude airborne gamma-ray spectrometry in Payne County, Oklahoma: Econ. Geol., v. 68, p. 1297-1312.

Saunders, D. F., and Potts, M. J., 1978, Manual for the application of NURE 1974-1977 aerial gamma-ray spectrometer data: Dept. of Energy, Rept. GJBX-13 (78).

Ward, D. L., and Stromswold, D. C., 1978, Procedures and regulations for airport calibration pads, Walker Field, Grand Junction, Colorado: Bendix Field Engineering Corporation, Report GJBX-38 (78).

Table 1 - Mean Concentrations of uranium, thorium, and potassium for several representative classes (after Adams et al., 1959 and Kogan et al., 1971).

Rock Type	Uranium (ppm)		Thorium (ppm)		Potassium (%)	
	Average	Range	Average	Range	Average	Range
Ultrabasic	0.003	-	0.005	-	0.03	-
Basic	1.0	0.2-4.0	4.0	0.5-10.0	0.7	0.2-1.6
Intermediate	1.8	-	7.0	-	2.3	-
Granitic	3.0	1.0-7.0	12.0	1.0-25.0	2.5	1.6-4.8
Shale	3.7	1.5-5.5	12.0	8.0-18.0	2.2	1.3-3.5
Sandstone	0.5	0.2-0.6	1.7	0.7-2.0	1.0	0.6-3.2
Carbonates	2.2	0.1-9.0	1.7	0.1-7.0	0.25	0.0-1.6
Evaporites	0.1	-	0.4	-	0.1	-

Table 2 $^{238}_{92}U$ Decay Series
(after Crouthamel, 1969)

Isotope		Half-life	Radiation
Uranium	238	4.51×10^{9} yr	α, γ
Thorium	234	24.1 day	α, γ
Protactinium	234	6.7 hr	β, γ
Uranium	234	2.48×10^{5} yr	α, γ
Thorium	230	8×10^{4} yr	α, γ
Radium	226	1622 yr	α, γ
Radon	222	3.82 day	α, γ
Polonium	218	3.05 min	α, β
Astatine	218	1.35 sec	α
Radon	218	0.03 sec	α
Bismuth	214	19.7 min	β, α, γ
Polonium	214	1.64×10^{-4} sec	α
Lead	214	26.8 min	β, γ
Lead	210	21 yr	β, γ
Bismuth	210	5 day	β
Polonium	210	138.4 day	α, γ
Thallium	210	1.3 min	β, γ
Thallium	206	4.2 min	β
Lead	206	stable	—

Table 3 - Principal Lines of the $^{238}_{92}U$ Gamma-ray Spectrum (after Crouthamel, 1969)

Isotope	Half-life	Energy of Each Quantum (MeV)	Number of Quanta per Decay Event
$^{214}_{83}Bi$	19.7 min	2.204	0.052
		1.764	0.163
		1.120	0.166
		0.609	0.417
$^{214}_{82}Pb$	26.8 min	0.352	0.377

Table 4 - $^{232}_{90}Th$ Decay Series
(after Crouthamel, 1969)

Isotope		Half-life	Radiation
Thorium	232	1.4×10^{10} yr	α, γ
Radium	228	5.7 yr	β, γ
Actinium	228	6.1 hr	β, γ
Thorium	228	1.91 yr	α, γ
Radium	224	3.64 day	α, γ
Radon	220	51 sec	α, γ
Polonium	216	0.16 sec	α
Lead	212	10.6 hr	β, γ
Bismuth	212	60.6 min	β, α, γ
Polonium	212	0.3×10^{-6} sec	α
Thallium	208	3.1 min	β, γ
Lead	208	stable	-

Table 5 - Principal Lines of the $^{232}_{90}Th$ Gamma-ray Spectrum
(after Crouthamel, 1969)

Isotope	Half-life	Energy of Each Quantum (MeV)	Number of Quanta per Decay Event
$^{228}_{89}Ac$	6.1 hr	0.960	0.100
$^{212}_{82}Pb$	10.6 hr	0.239	0.470
$^{208}_{81}Tl$	3.1 min	2.620	0.337
		0.583	0.293

Table 6.

Half-Thicknesses for Air, Water, and Rock

Energy (MeV)	Air (m)	Water (cm)	Rock (cm)
0.01	1.2	0.1	0.01
0.10	38.1	4.1	1.7
1.0	90.6	9.8	4.6
2.0	129.3	14.1	6.6
3.0	161.1	17.5	8.1

Table 7 Compton Scattering (•⟶)

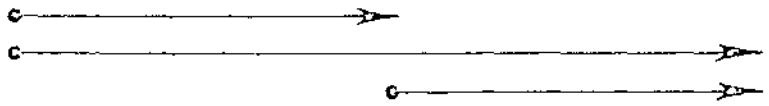

Nuclide	^{208}Tl	^{214}Bi	^{40}K
Indicator	Th	U	K
Energy	2.62 MeV	1.76 MeV	1.46 MeV

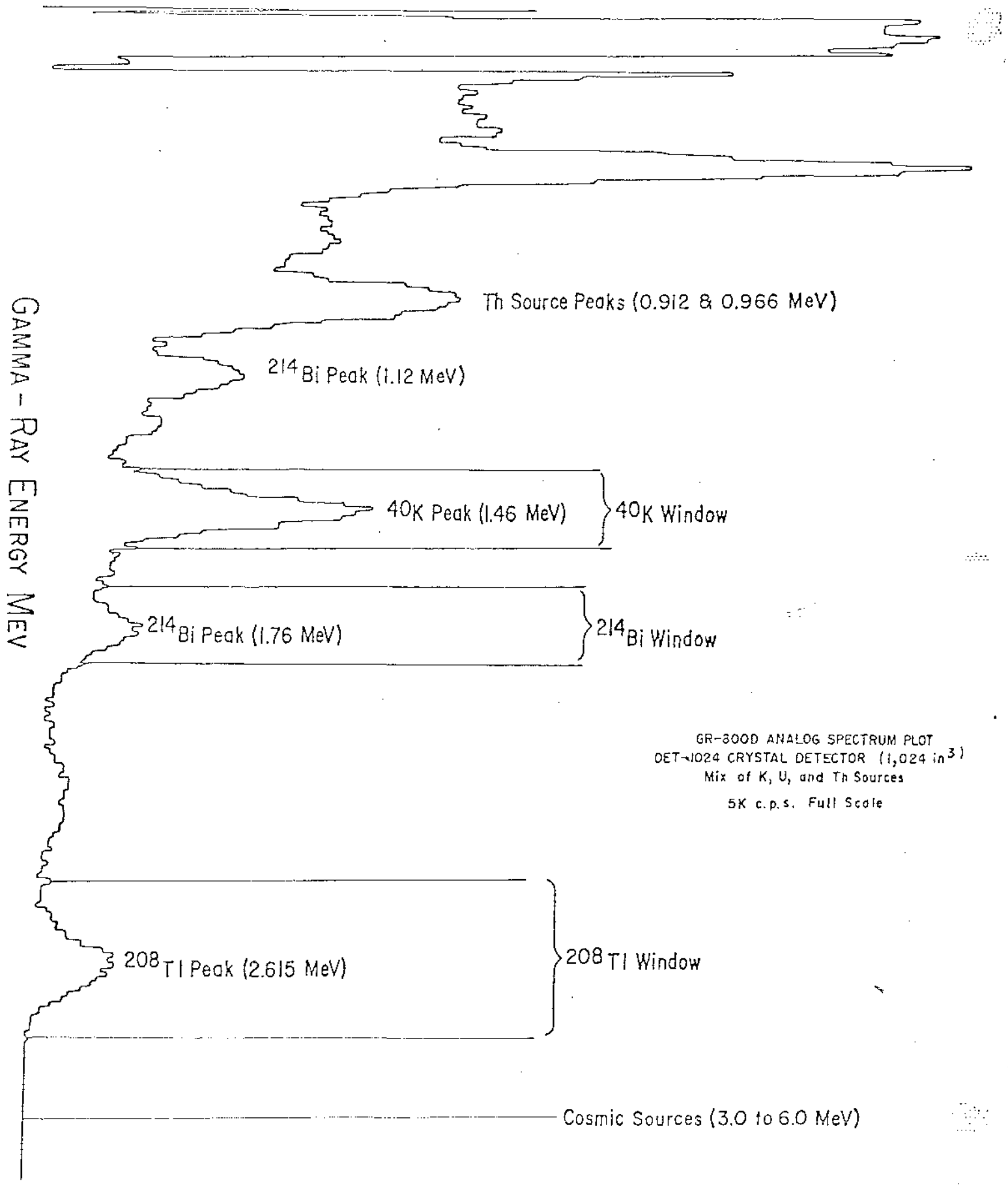
RELATIVE GAMMA-RAY COUNTS
GAMMA - RAY ENERGY MEV
Th Source Peaks (0.912 & 0.966 MeV)
214Bi Peak (1.12 MeV)
40K Peak (1.46 MeV)
40K Window
214Bi Peak (1.76 MeV)
214Bi Window
208Tl Peak (2.615 MeV)
208Tl Window
Cosmic Sources (3.0 to 6.0 MeV)
GR-800D ANALOG SPECTRUM PLOT
DET-1024 CRYSTAL DETECTOR (1,024 in3)
Mix of K, U, and Th Sources
5K c.p.s. Full Scale

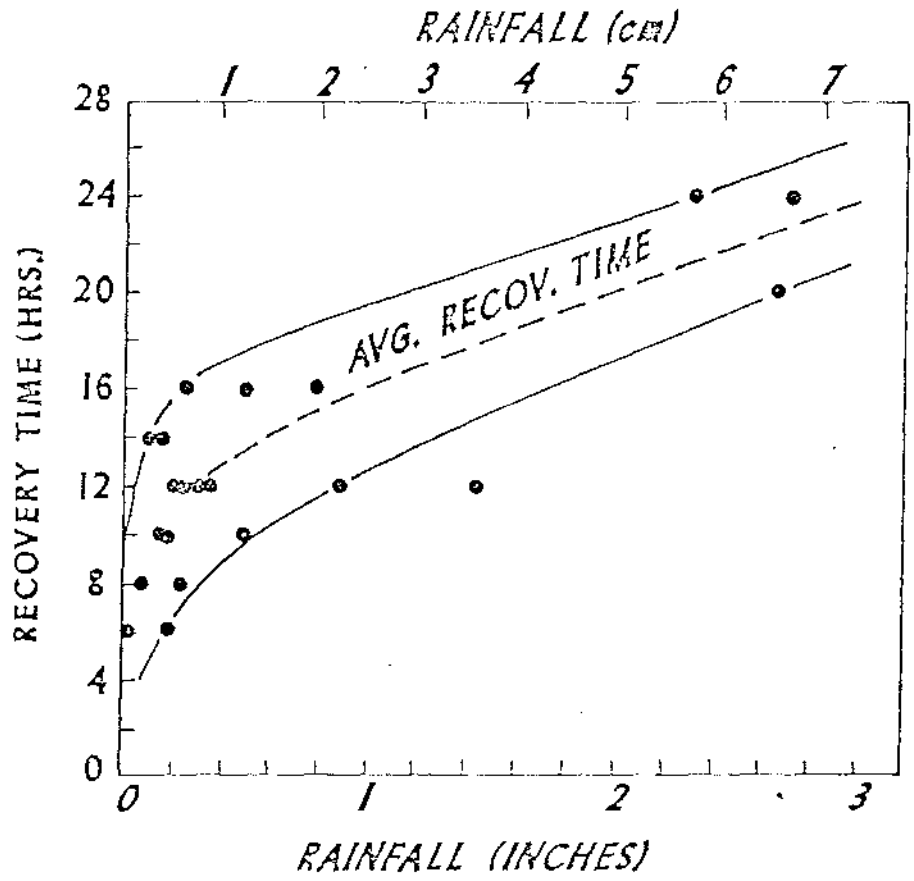
RAINFALL (cm)
1
2
3
4
5
6
7
28
24
20
16
12
8
4
0
RECOVERY TIME (HRS.)
AVG. RECOV. TIME
0
1
2
3
RAINFALL (INCHES)

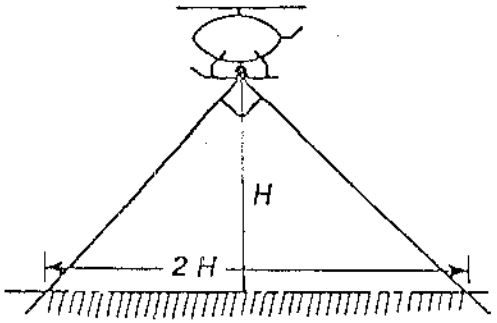

a) NORMAL COUNT RATE

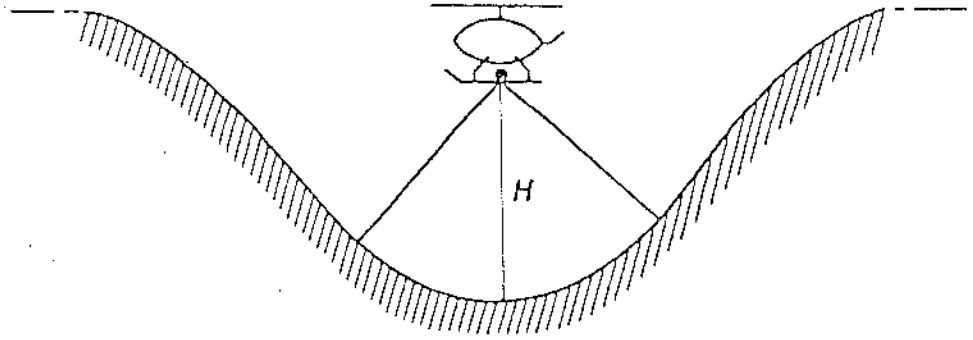

b) HIGH COUNT RATE

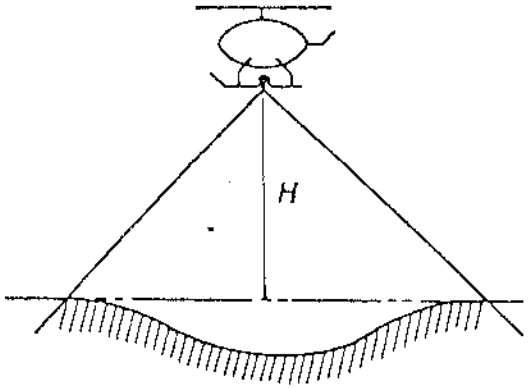

c) LOW COUNT RATE

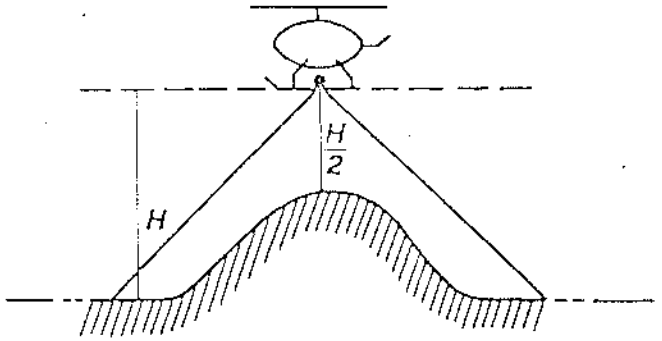

d) HIGH COUNT RATE

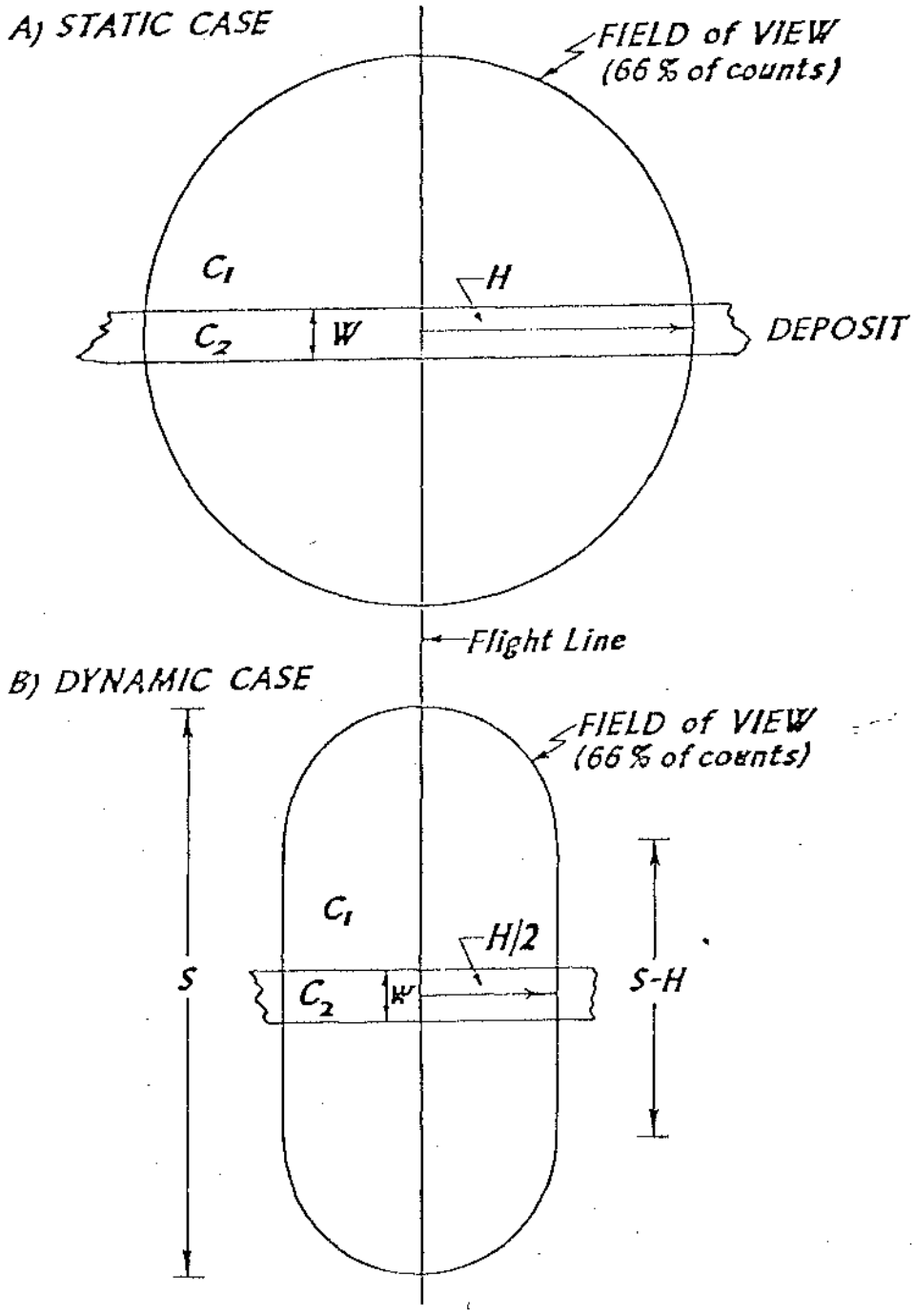
A) STATIC CASE
FIELD of VIEW
(66 % of counts)
C_1
H
C_2
W
DEPOSIT
Flight Line
B) DYNAMIC CASE
FIELD of VIEW
(66 % of counts)
C_1
H/2
S
C_2
W
S-H

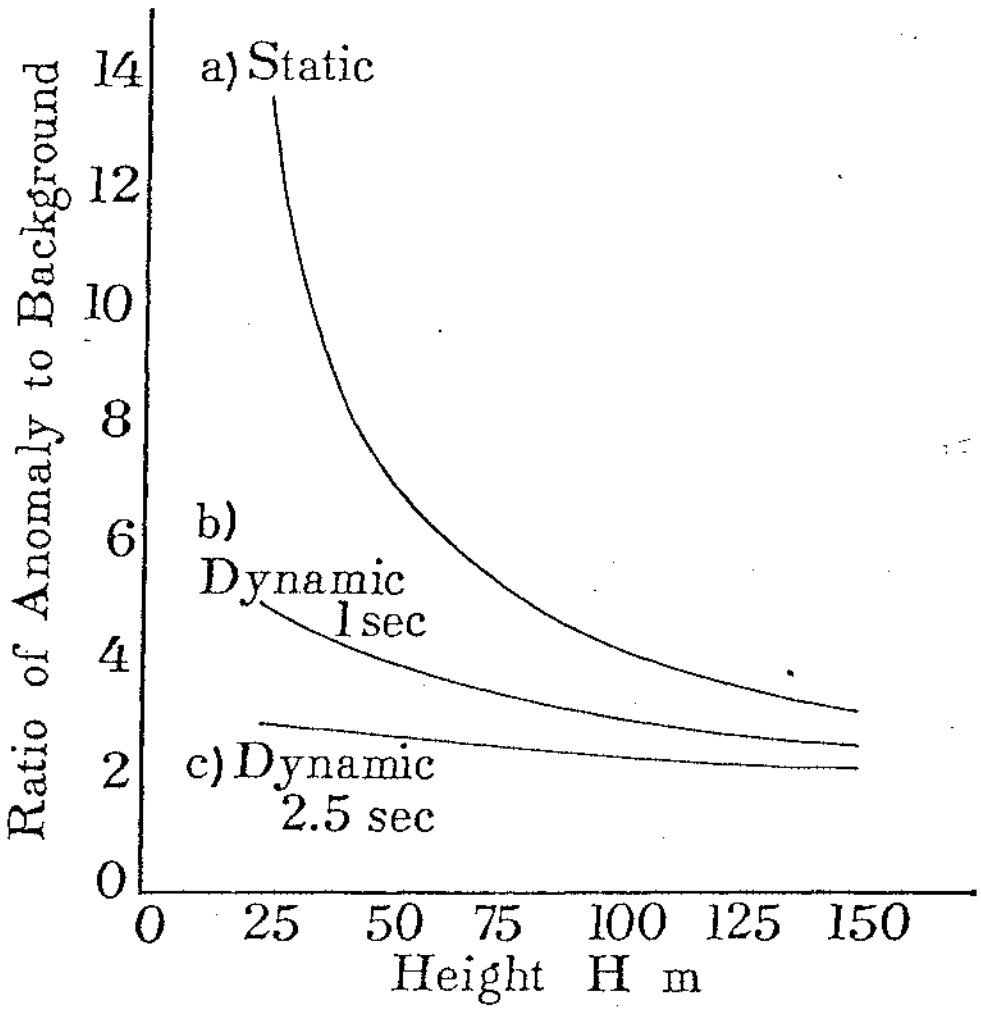
Ratio of Anomaly to Background
14
12
10
8
6
4
2
0
a) Static
b)
Dynamic
1 sec
c) Dynamic
2.5 sec
0
25
50
75
100
125
150
Height H m

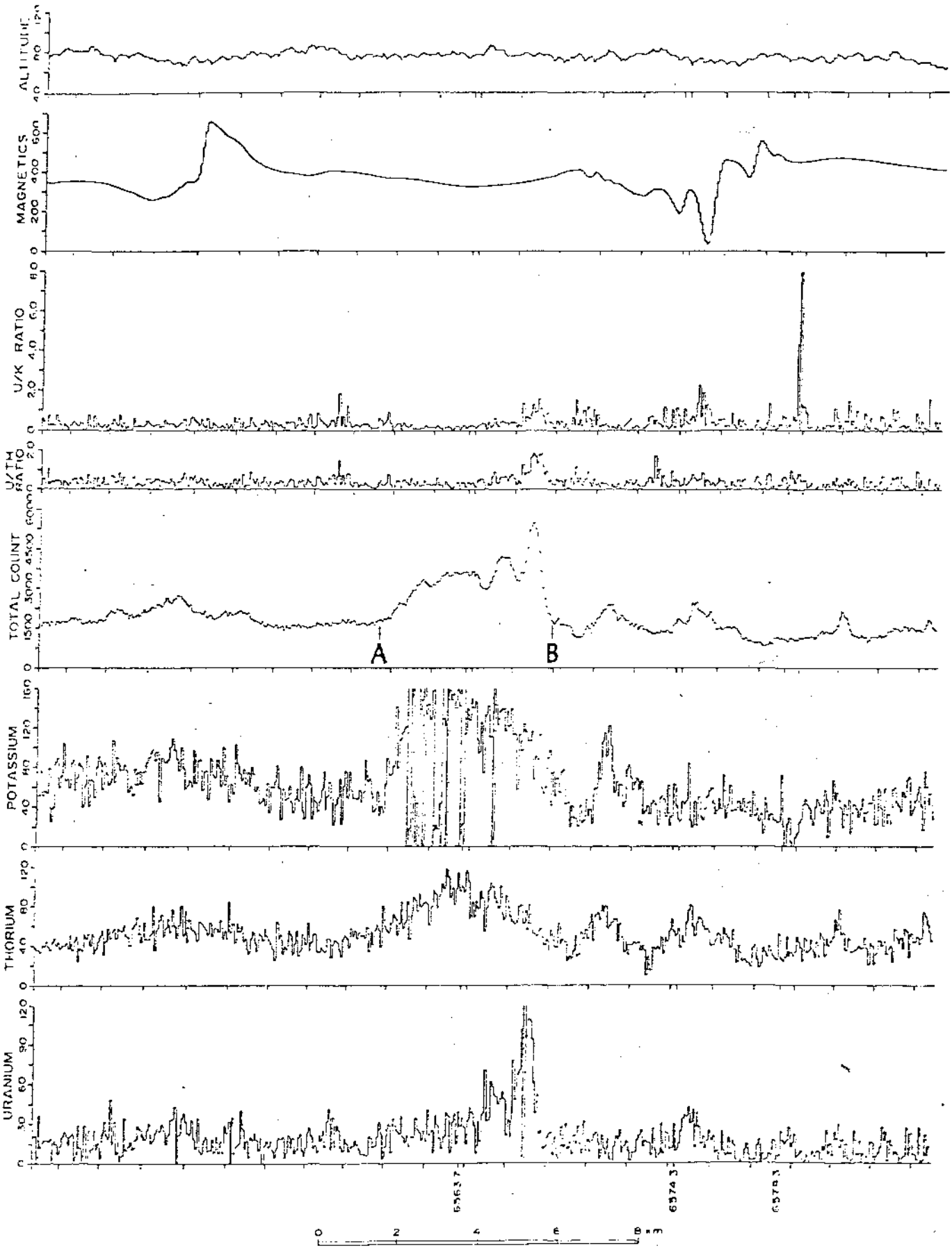
ALTITUDE
MAGNETICS
U/K RATIO
U/TH RATIO
TOTAL COUNT
A
B
POTASSIUM
THORIUM
URANIUM
6563.7
6574.3
6578.3
0 2 4 6 8 km

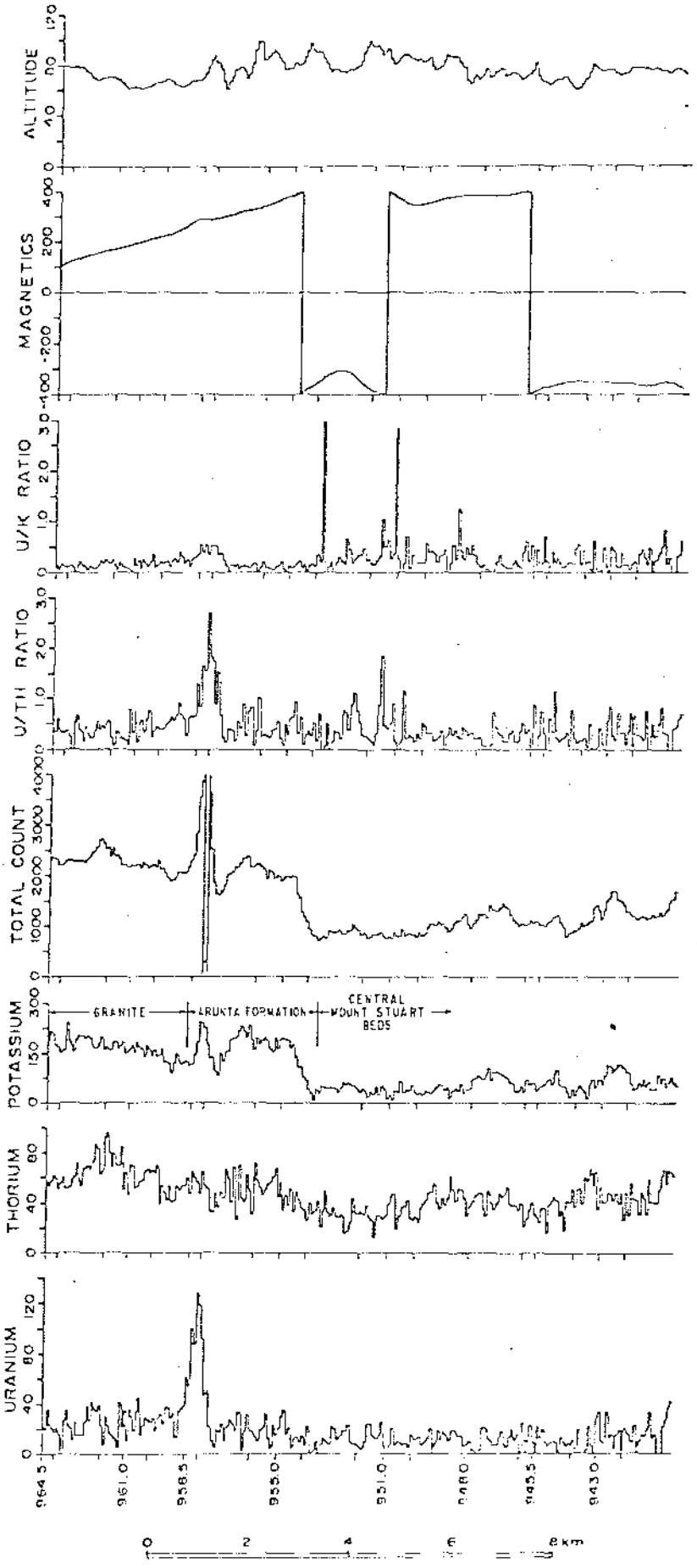
ALTITUDE
MAGNETICS
U/K RATIO
U/TH RATIO
TOTAL COUNT
POTASSIUM
GRANITE
ARUNTA FORMATION
CENTRAL MOUNT STUART BEDS
THORIUM
URANIUM
964.5
961.0
958.5
955.0
951.0
948.0
945.5
943.0
0 2 4 6 8 km